

Temporal and Interactive Modeling for Efficient Human-Human Motion Generation

Yabiao Wang^{1,2*}, Shuo Wang^{2*}, Jiangning Zhang², Ke Fan³,
Jiafu Wu², Zhengkai Jiang², Yong Liu^{1†}

¹Zhejiang University ²Youtu Lab, Tencent ³Shanghai Jiao Tong University
<https://aigc-explorer.github.io/TIM-page/>

Abstract

Human-human motion generation is essential for understanding humans as social beings. Although several transformer-based methods have been proposed, they typically model each individual separately and overlook the causal relationships in temporal motion sequences. Furthermore, the attention mechanism in transformers exhibits quadratic computational complexity, significantly reducing their efficiency when processing long sequences. In this paper, we introduce TIM (Temporal and Interactive Modeling), an efficient and effective approach that presents the pioneering human-human motion generation model utilizing RWKV. Specifically, we first propose Causal Interactive Injection to leverage the temporal properties of motion sequences and avoid non-causal and cumbersome modeling. Then we present Role-Evolving Mixing to adjust to the ever-evolving roles throughout the interaction. Finally, to generate smoother and more rational motion, we design Localized Pattern Amplification to capture short-term motion patterns. Extensive experiments on InterHuman demonstrate that our method achieves superior performance. Notably, TIM has achieved state-of-the-art results using only 32% of InterGen’s trainable parameters. Code will be available soon.

Introduction

Generating human motion is a critical challenge in the field of generative computer vision, with significant implications for computer animation (Parent 2012; Magnenat-Thalmann et al. 1985), game development (Urbain 2010; Bethke 2003), and robotic control (Saridis 1983; Wang et al. 2023a). In recent years, there has been remarkable advancements in human motion generation, driven by various user-specified conditions such as action categories (Petrovich, Black, and Varol 2021; Guo et al. 2020), speeches (Ao et al. 2022; Habibie et al. 2022), and natural language prompts (Pinyoanun-tapong et al. 2024; Guo et al. 2024). Despite these significant strides, most existing motion diffusion models are designed primarily for single-person scenarios, thereby neglecting a crucial element of human motion: the complex and dynamic interactions between individuals.

Although several transformer-based methods for human-human interaction have been proposed (Tanaka and Fuji-

wara 2023; Liang et al. 2024), they generally involve modeling each individual separately before integrating their interactions, a process that is both cumbersome and time-consuming, as illustrated in Fig. 3(a). Moreover, the attention mechanism in transformers exhibits quadratic computational complexity, significantly reducing their efficiency when processing long sequences.

Previous methods fail to account for the intrinsic properties of motion during human-human interaction. As shown in Fig. 1, the interaction process exhibits specific properties. First, the motion sequences are temporally causal, *i.e.*, motions at the current moment are co-determined by motions at previous time steps. Second, interactive motions can be categorized as active or passive, with passive motions typically influenced by active motions. Moreover, the roles of active and passive participants frequently change, as exemplified by the active pusher switching from the first person to the second person in Fig. 1. Overall, motion and natural language share some similar properties, highlighting the necessity of exploring efficient and effective methods utilizing RNNs in human-human interaction.

In recent advancements, models like RWKV (Peng et al. 2023) and Mamba (Gu and Dao 2023) have gained traction as efficient solutions for processing extensive textual data while maintaining capabilities comparable to transformers. These cutting-edge models manage long-range dependencies and offer significantly lower linear complexity. Nevertheless, there has been no research investigating the use of these models for generating human-human motion.

In this paper, we introduce **Temporal and Interactive Modeling (TIM)**, a pioneering approach that applies RWKV to human-human motion generation. First, due to the temporal causal properties of motion sequences, we propose Causal Interactive Injection, which models the two single-person motion sequences as a causal interaction sequence and then injects it into the RWKV layer. Second, we incorporate Role-Evolving Mixing to adapt to the dynamic adjustment of "active" and "passive" roles in the interaction process based on the semantics of the text and the context of the motion. Finally, we propose Localized Pattern Amplification, which captures short-term motion patterns for each individual separately, resulting in smoother and more logical motion generation. In summary, the primary contributions of this paper are outlined as follows:

*Equal contributions.

†Corresponding author.



The first person suddenly pushes the other one. The second person takes a step back, then forcefully pushes the first person. The first person was knocked down.

Figure 1: Illustration of the intrinsic properties of motion in the interaction process. First, current motion is co-determined by motions at previous time steps, which shows causality. Second, motion typically initiates with active and passive roles, and the roles of active and passive participants frequently change.

- We introduce TIM, which innovatively applies RWKV to address human-human motion generation tasks and has been proven to be an efficient and effective alternative.
- We propose Causal Interactive Injection to utilize the temporal properties of motion sequences and Role-Evolving Mixing to adapt to the changes in roles during interactions. Moreover, we design Localized Pattern Amplification, which captures short-term motion patterns.
- We conduct extensive experiments on the standard human-human motion generation dataset, InterHuman, and the results demonstrate the efficacy and generalizability of our proposed methods. Notably, our method has achieved state-of-the-art results using only 32% of InterGen’s trainable parameters.

Related Works

Single-Person Human Motion Generation. Creating human motion is vital for applications such as 3D modeling and robot manipulation. The primary approach, known as the Text-to-Motion task, involves learning a unified latent space for both language and motion.

Autoencoders have been widely adopted in human motion generation. MotionCLIP (Tevet et al. 2022a) leverages the shared text-image latent space learned by CLIP (Radford et al. 2021) to integrate the semantic knowledge from CLIP into the human motion manifold effectively. TEMOS (Petrovich, Black, and Varol 2022) and T2M (Guo et al. 2022) combine a Transformer-based VAE with a text encoder to generate motion sequences based on text descriptions. AttT2M (Zhong et al. 2023) and TM2D (Gong et al. 2023) integrate a body-part spatio-temporal encoder into VQ-VAE (Van Den Oord, Vinyals et al. 2017) to improve the learning of discrete latent space, thereby increasing its expressiveness. T2M-GPT (Zhang et al. 2023a) redefines text-driven motion generation as a next-index prediction task and proposes a framework based on VQ-VAE and Generative Pretrained Transformer (GPT) for motion generation.

Recently, diffusion-based generative modeling has been gaining attention. MotionDiffuse (Zhang et al. 2024a) and MDM (Tevet et al. 2022b) represent pioneering frameworks for text-driven motion generation using diffusion models. MotionDiffuse exhibits several desirable properties, such as probabilistic mapping, realistic synthesis, and multi-level manipulation. MDM aims to predict motion itself directly and additionally incorporates a geometric loss to boost

the model’s performance. Instead of employing a diffusion model to link raw motion sequences with conditional inputs, MLD (Chen et al. 2023) further utilizes the latent diffusion model to substantially reduce the training and inference costs. ReMoDiffuse (Zhang et al. 2023b) introduces an improvement mechanism based on dataset retrieval to enhance the denoising process of Diffusion. FineMoGen (Zhang et al. 2024b) further presents a diffusion-based model that can synthesize fine-grained motions.

Multi-Person Human Motion Generation. As multi-person motion synthesis involves the interactive dynamics between multiple individuals, it is more challenging than single-person motion generation. Early work typically relied on motion graphs and momentum-based inverse kinematics to model human joints. Recently, some advanced methods have been proposed. ComMDM (Shafir et al. 2023) fine-tunes a pre-trained text-to-motion diffusion model using a small scale of two human motions. RIG (Tanaka and Fujiwara 2023) converts the text of asymmetric interactions into both active and passive voice to maintain consistent textual context for each individual. To complete the interaction process by manipulating the joints of two individuals to specific positions, InterControl (Wang et al. 2023b) employs a Large Language Model (LLM) to generate movement plans for the two individuals by designing prompts. InterGen (Liang et al. 2024) initially introduces a large-scale, text-annotated two-person motion dataset named InterHuman. Building on this dataset, it proposes a diffusion model with shared weights and multiple regularization losses.

Receptance Weighted Key Value. The Receptance Weighted Key Value (RWKV) model, originally developed for NLP tasks, is emerging as an efficient alternative to Transformers. RWKV provides two primary advantages over the Transformer model. Firstly, RWKV (Peng et al. 2023) introduces a WKV attention mechanism that establishes long-range dependencies with linear computational complexity, while at the same time addressing the quadratic computational complexity of self-attention in Transformers. Secondly, RWKV incorporates a token shift layer to capture local context, which is often overlooked by the Transformer. Recent studies indicate that RWKV can match or even exceed both Transformers (Vaswani 2017) and Mamba (Gu and Dao 2023) in NLP tasks. Recently, Vision-RWKV (Duan et al. 2024) has adapted RWKV to vision tasks, showing superior performance compared to vision

transformers with lower computational complexity. Building on RWKV and Vision-RWKV, several RWKV-based models have been developed for various tasks, such as DiffusionRWKV (Fei et al. 2024) for image generation, RWKV-SAM (Yuan et al. 2024) for segmentation tasks, Point-RWKV (He et al. 2024) for 3D point cloud learning, RWKV-CLIP (Gu et al. 2024) for vision-language representation learning and Restore-RWKV (Yang et al. 2024) for medical image restoration. However, few studies have assessed the performance of RWKV in human motion generation tasks. To address this, we propose TIM, an efficient and effective approach that presents the pioneering human-human motion generation model utilizing RWKV.

Preliminary

RWKV

RWKV (Peng et al. 2023) introduced enhancements to the traditional RNN architecture (Hochreiter and Schmidhuber 1997), enabling parallel computation during training while maintaining RNN-like behavior during inference. This involves refining the linear attention mechanism and creating the RWKV mechanism. Typically, the RWKV model comprises an input layer, multiple stacked residual blocks, and an output layer. Each residual block includes time mixing and channel mixing sub-blocks.

The time mixing Block is designed to enhance the modeling of dependencies and patterns within a sequence. This is accomplished by substituting the conventional weighted sum calculation in an attention mechanism with hidden states. The time mixing block effectively propagates and updates information across sequential steps using hidden states, and this updating process can be described as follows:

$$\begin{aligned} q_t &= (\mu_q \odot x_t + (1 - \mu_q) \odot x_{t-1}) \cdot W_q, \\ k_t &= (\mu_k \odot x_t + (1 - \mu_k) \odot x_{t-1}) \cdot W_k, \\ v_t &= (\mu_v \odot x_t + (1 - \mu_v) \odot x_{t-1}) \cdot W_v, \\ o_t &= (\sigma(q_t) \odot h(k_t, v_t)) \cdot W_o, \end{aligned} \quad (1)$$

where q_t , k_t , and v_t are derived by linearly interpolating between the current input and the previous input. The interpolation, guided by the token shift parameter μ , ensures smooth and coherent token representations. Furthermore, a non-linear activation function σ is applied to q_t , and the resulting value is combined with the hidden states $h(k_t, v_t)$ through element-wise multiplication. The hidden states can be calculated as follows:

$$\begin{aligned} p_t &= \max(p_{t-1}, k_t), \\ h_t &= \frac{\exp(p_{t-1} - p_t) \cdot a_{t-1} + \exp(k_t - p_t) \cdot v_t}{\exp(p_{t-1} - p_t) \cdot b_{t-1} + \exp(k_t - p_t)}, \end{aligned} \quad (2)$$

where a_0, b_0, p_0 are zero-initialized. Intuitively, the hidden states are determined recursively, with the vector p acting as the reset gate throughout this process.

The channel mixing Block is designed to enhance the outputs of the time mixing block, which can be expressed as

follows:

$$\begin{aligned} r_t &= (\mu_r \odot o_t + (1 - \mu_r) \odot o_{t-1}) \cdot W_r, \\ z_t &= (\mu_z \odot o_t + (1 - \mu_z) \odot o_{t-1}) \cdot W_z, \\ \hat{x}_t &= \sigma(r_t) \odot (\max(z_t, 0)^2) \cdot W_v, \end{aligned} \quad (3)$$

The output o_t encapsulates historical information up to time t , with the interpolation weight μ being derived from o_t and o_{t-1} . This is akin to the time mixing block, which also improves the representation of historical information.

Motion Diffusion Model

Diffusion probabilistic models represent a breakthrough in motion generation by progressively reducing noise from a Gaussian distribution to a target data distribution $p(x)$ through a T-step learned Markov process (Ho, Jain, and Abbeel 2020; Dhariwal and Nichol 2021). Suppose that T is the motion length and $\{x_t\}_{t=1}^T$ is the motion sequence and z_t is the corresponding noising motion, we define the trainable diffusion models with a denoiser $\epsilon_\theta(z_t, t)$ that iteratively refines random noise into a motion sequence $\{\hat{x}_t\}_{t=1}^T$. Given an input condition c , typically a descriptive sentence $w^{1:N} = \{w_i\}_{i=1}^N$, and the motion representation that integrates 3D joint rotations, positions, velocities, and foot contact, we employ the frozen CLIP (Radford et al. 2021) text encoder τ_θ^w to obtain projected text embeddings $\tau_\theta^w(w^{1:N}) \in \mathbb{R}^{1 \times d}$. This allows the conditional denoiser to be defined as $\epsilon_\theta(z_t, t, \tau_\theta(c))$. Finally, the motion diffusion model is trained with an objective that minimizes the MSE between the true and predicted noise, thereby enabling efficient and high-quality motion generation.

Method

In this section, we introduce the details of our proposed TIM, which consists of three components: (1) Causal Interactive Injection; (2) Role-Evolving Scanning; (3) Localized Pattern Amplification Module. Fig. 4 shows the overall architecture of TIM.

Causal Interactive Injection

The perception of self-motion and the perception of the other’s motion are two important elements of human-human interaction. Previous methods (Liang et al. 2024) usually require two network layers as well as four steps to complete the process of human-human interaction, as shown in Fig. 3(a). Specifically, we model two single-person motion sequences as $\{x_a, x_b\}$, where $x_a = \{x_a^i\}_{i=1}^L$ and $x_b = \{x_b^i\}_{i=1}^L$ are respective sequences of motion, and L is the length of the sequence. The process of human-human interaction can be expressed as:

$$\begin{aligned} x'_a &= \text{Self_Layer}(x_a), \\ x'_b &= \text{Self_Layer}(x_b), \\ x''_a &= \text{Cross_Layer}(x'_a, x'_b), \\ x''_b &= \text{Cross_Layer}(x'_b, x'_a), \end{aligned} \quad (4)$$

where `Self_Layer` (e.g. self-attention of the transformer) is responsible for extracting the intrinsic information of a single person’s motion and `Cross_Layer` (e.g. cross-attention

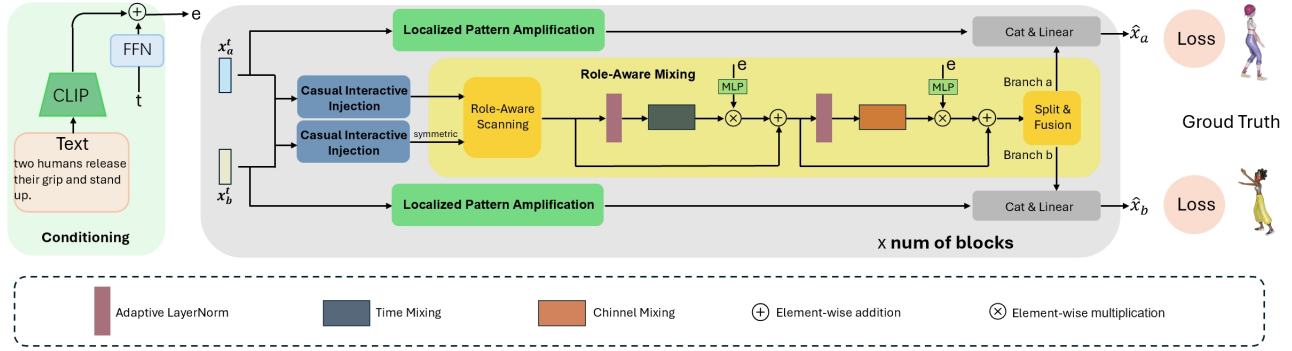


Figure 2: The overall framework of our TIM. We contribute three primary technical designs. First, we propose Causal Interactive Injection to utilize the temporal properties of motion sequences. Then we present Role-Evolving Mixing to adjust to the ever-evolving roles during interaction. Finally, we design Localized Pattern Amplification to capture short-term motion patterns.

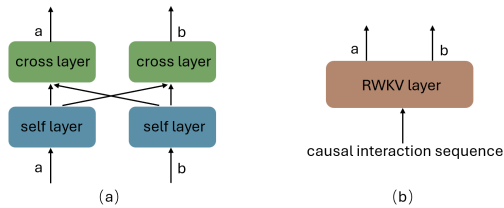


Figure 3: (a) shows the structure which models separately for two persons. (b) shows the structure of causal modeling.

of the transformer) aims to exchange information about the motion states of two individuals.

However, the above non-causal method is cumbersome and facilitates human-human interaction indirectly through multiple steps rather than straightforwardly. Considering the causal properties of motions and natural language, we propose Causal Interactive Injection, which takes advantage of RNNs to achieve human-human interaction with only requires one network layer and one step.

Since the motions of two individuals at the current time step are jointly determined by their motions at previous time steps, we model the two single-person motion sequences as a causal interaction sequence $x = \{x_k^{i//2}\}_{i=1}^{2L}$, where L is the length of the sequence, the symbol $//$ denotes division followed by rounding up and k can be acquired as follows:

$$k = \begin{cases} a, & i \% 2 = 1. \\ b, & i \% 2 = 0. \end{cases} \quad (5)$$

RWKV (Peng et al. 2023) has a natural advantage in processing temporal sequences and is able to process long sequences with linear efficiency. To better utilize causal interaction sequences, we inject them into the RWKV_Layer as follows:

$$x' = \text{RWKV_Layer}(x), \quad (6)$$

Then we can separate the motion embeddings of the two individuals from x' according to Eq. (5).

As shown in Fig. 3(b), we employ only one layer (RWKV_Layer) and one step (Eq. (6)) to achieve human-human interaction through Causal Interactive Injection.

Role-Evolving Mixing

As noted in (Cai et al. 2024), there exists an intrinsic order in human interaction, *e.g.*, "shaking hands" typically initiates with one person extending a hand first, which means that interactive motion can be categorized as active or passive. Some methods (Tanaka and Fujiwara 2023) splits the text description into active and passive voices. However, the "active" and "passive" roles constantly swap between characters as the interaction progresses, as shown in Fig. 1. To avoid redundant text preprocessing and adapt to the constant change of roles, we design Role-Evolving Mixing, which is efficient and effective.

For the causal interaction sequence x defined in Causal Interactive Injection, it is obvious that x_a and x_b represent the active sequence and passive sequence, respectively due to the temporal properties of RNNs (*e.g.*, RWKV). The above assumption of active and passive motions is not always in line with the real order. To cope with the changing roles, we re-model the interactive motion sequences as a symmetric causal interaction sequence $x_{sym} = \{x_{k'}^{i//2}\}_{i=1}^{2L}$, where the symbol $//$ is defined as division followed by rounding up and k' can be acquired as follows:

$$k' = \begin{cases} b, & i \% 2 = 1. \\ a, & i \% 2 = 0. \end{cases} \quad (7)$$

Given that the causal interaction sequence $x \in \mathbb{R}^{2L \times C}$ and the symmetric causal interaction sequence $x_{sym} \in \mathbb{R}^{2L \times C}$, where L is the length of the sequence and C is the dimension of motion embedding, we can acquire the final interaction sequence $x_r \in \mathbb{R}^{2L \times 2C}$ through Role-Evolving Scanning as:

$$x_r = \text{Concat}(x, x_{sym}). \quad (8)$$

To better realize the dynamic transformation of roles according to the contextual semantics, and motivated by (Fei et al. 2024), we propose adaptive mixing modulation that utilizes RWKV in human interaction tasks. Given the condition embedding e , which mixes text and denoising times-

tamp t , the adaptive mixing modulation operates as:

$$\begin{aligned} Scale_t &= \psi_{st}(e), & Offs_t &= \psi_{ot}(e), \\ Scale_c &= \psi_{sc}(e), & Offs_c &= \psi_{oc}(e), \\ Scale'_t &= \psi_{st'}(e), & Scale'_c &= \psi_{sc'}(e), \end{aligned} \quad (9)$$

$$\begin{aligned} x_t &= x_r + Scale'_t \odot TM(Scale_t \odot LN(x_r, e) + Offs_t), \\ x_c &= x_t + Scale'_c \odot CM(Scale_c \odot LN(x_t, e) + Offs_c), \end{aligned}$$

where $\psi_{st}, \psi_{ot}, \psi_{sc}, \psi_{oc}, \psi_{st'}, \psi_{sc'}$ denote six different linear projections, LN is adaptive layer norm used in (Zhang et al. 2024a), \odot denotes element-wise multiplication, and TM and CM represent time mixing and channel mixing, respectively.

After obtaining the output $x_c \in \mathbb{R}^{2L \times 2C}$ from the adaptive mixing modulation, we first divide it at the channel level into causal interaction embeddings and symmetric causal interaction embeddings. According to Eq. (5) and Eq. (7), we can obtain the two individuals' splitting embeddings twice. Then we merge the embeddings of the two individuals to obtain the final global motion embeddings x_a^g and x_b^g . The overall process is as follows:

$$\begin{aligned} x_{a1}, x_{b1} &= \text{Split}(x_c[:, : C]), \\ x_{b2}, x_{a2} &= \text{Split}(x_c[:, C :]), \\ x_a^g &= x_{a1} \oplus x_{a2}, \\ x_b^g &= x_{b1} \oplus x_{b2}, \end{aligned} \quad (10)$$

where \oplus denotes element-wise sum.

By utilizing Role-Evolving Mixing to make two humans act as both active and passive roles, the network can dynamically adjust the roles of the two humans based on the semantics of the text and the context of the motion.

Localized Pattern Amplification

Transformers and RNNs excel in global modeling and capturing long-range dependencies but tend to overlook local semantic information. Additionally, Causal Interactive Injection and Role-Evolving Mixing mainly model the overall motion based on the causality of the interactions but neglect to focus on localized motion patterns. To address this issue, we propose Localized Pattern Amplification, which summarizes short-term motion patterns for each person individually while generating smoother and more rational motion.

Specifically, we utilize 1-D convolution layers and the residual structure to realize Localized Pattern Amplification. Given that the condition embedding e and two single-person motion sequences x_a and x_b , the local motion embedding for x_a can be expressed as:

$$\begin{aligned} x_a^1 &= \text{Conv}_3(LN(x_a, e)), \\ x_a^2 &= \text{Conv}_1(LN(x_a^1, e)), \\ x_a^l &= x_a + x_a^2, \end{aligned} \quad (11)$$

where Conv_k denotes the 1-D convolution with kernel size k and LN is the adaptive layer norm used in (Zhang et al. 2024a). The process for x_b is the same as for x_a and they share network weights.

Once we obtain the outputs $\{x_a^g, x_b^g\}$ of Role-Evolving Mixing and the output $\{x_a^l, x_b^l\}$ from the convolution block,

global embeddings and local embeddings are aggregated through concatenation along the channel dimension, followed by a linear layer to restore the original channels, resulting in the final outputs $\{x_a^{final}, x_b^{final}\}$:

$$\begin{aligned} x_a^{final} &= \text{Linear}(\text{Concat}(x_a^g, x_a^l)), \\ x_b^{final} &= \text{Linear}(\text{Concat}(x_b^g, x_b^l)). \end{aligned} \quad (12)$$

Then the final outputs are fed into the next encoder block or the final decoder layer.



Figure 4: The structure of Localized Pattern Amplification.

Objective Function

We adopt the common losses for each single-person motion, including the foot contact loss \mathcal{L}_{foot} and joint velocity loss \mathcal{L}_{vel} . Additionally, we use the same regularization loss functions as InterGen (Liang et al. 2024), including the bone length loss \mathcal{L}_{BL} , the masked joint distance map loss \mathcal{L}_{DM} , and the relative orientation loss \mathcal{L}_{RO} . For more details about the regularization losses, we refer readers to InterGen. Finally, the overall loss is defined as:

$$\begin{aligned} \mathcal{L}_{motion} &= \lambda_{vel} \mathcal{L}_{vel} + \lambda_{foot} \mathcal{L}_{foot} + \lambda_{BL} \mathcal{L}_{BL} \\ &\quad + \lambda_{DM} \mathcal{L}_{DM} + \lambda_{RO} \mathcal{L}_{RO}, \end{aligned} \quad (13)$$

where the hyper-parameters $\lambda_{vel}, \lambda_{foot}, \lambda_{BL}, \lambda_{DM}, \lambda_{RO}$ are the same as InterGen.

Experiments

Experimental Setup

Datasets. We assess our proposed framework using the InterHuman (Liang et al. 2024) dataset, which is the first dataset to feature text annotations for two-person motions. This dataset includes 6,022 motions spanning various categories of human actions, and is labeled with 16,756 unique descriptions made up of 5,656 distinct words.

Evaluation metrics. We employ the same evaluation metrics as InterGen (Liang et al. 2024), which are as follows: (1) *Frechet Inception Distance (FID)*: measures the latent distribution distance between the generated dataset and the real dataset. (2) *R-Precision*: assesses text-motion matching, indicating the probability that the real text appears in the Top- k ($k=1, 2, 3$) after sorting. (3) *Diversity*: measures motion diversity in the generated motion dataset. (4) *Multimodality (MModality)*: gauges diversity within the same text. (5) *Multi-modal distance (MM Dist)*: measures the distance between motions and text features.

Implementation Details. We configure our TIM model with 5 blocks. The dimension of motion embedding is set to 512, and each block has 16 attention heads per RWKV layer. We use a frozen CLIP-ViT-L/14 model as the text encoder. During training, the number of diffusion timesteps

Methods	R Precision \uparrow			FID \downarrow	MM Dist \downarrow	Diversity \rightarrow	MModality \uparrow
	Top 1	Top 2	Top 3				
TEMOS (Petrovich, Black, and Varol 2022)	0.224 \pm .010	0.316 \pm .013	0.450 \pm .018	17.375 \pm .043	5.342 \pm .015	6.939 \pm .071	0.535 \pm .014
T2M (Guo et al. 2022)	0.238 \pm .012	0.325 \pm .010	0.464 \pm .014	13.769 \pm .072	4.731 \pm .013	7.046 \pm .022	1.387 \pm .076
MDM (Tevet et al. 2022b)	0.153 \pm .012	0.260 \pm .009	0.339 \pm .012	9.167 \pm .056	6.125 \pm .018	<u>7.602</u> \pm .045	2.355 \pm .080
ComMDM* (Shafir et al. 2023)	0.067 \pm .013	0.125 \pm .018	0.184 \pm .015	38.643 \pm .098	13.211 \pm .013	3.520 \pm .058	0.217 \pm .018
ComMDM (Shafir et al. 2023)	0.223 \pm .009	0.334 \pm .008	0.466 \pm .010	7.069 \pm .054	5.212 \pm .021	7.244 \pm .038	1.822 \pm .052
RIG (Tanaka and Fujiwara 2023)	0.285 \pm .010	0.409 \pm .014	0.521 \pm .013	6.775 \pm .069	4.876 \pm .018	7.311 \pm .043	2.096 \pm .065
InterGen (Liang et al. 2024)	<u>0.371</u> \pm .010	<u>0.515</u> \pm .012	<u>0.624</u> \pm .010	<u>5.918</u> \pm .079	<u>4.108</u> \pm .014	<u>7.387</u> \pm .029	<u>2.141</u> \pm .063
TIM(ours)	0.501 \pm .005	0.656 \pm .006	0.734 \pm .006	4.702 \pm .069	3.769 \pm .001	7.943 \pm .034	1.005 \pm .020

Table 1: **Quantitative evaluation on the InterHuman (Liang et al. 2024) test set.** We run all the evaluations 20 times. \pm indicates a 95% confidence interval. **Bold** indicates the best result, while underscore refers to the second best. ComMDM* indicates the ComMDM model fine-tuned in the original few-shot setting with 10 training samples and ComMDM indicates fine-tuned on the entire InterHuman training set.

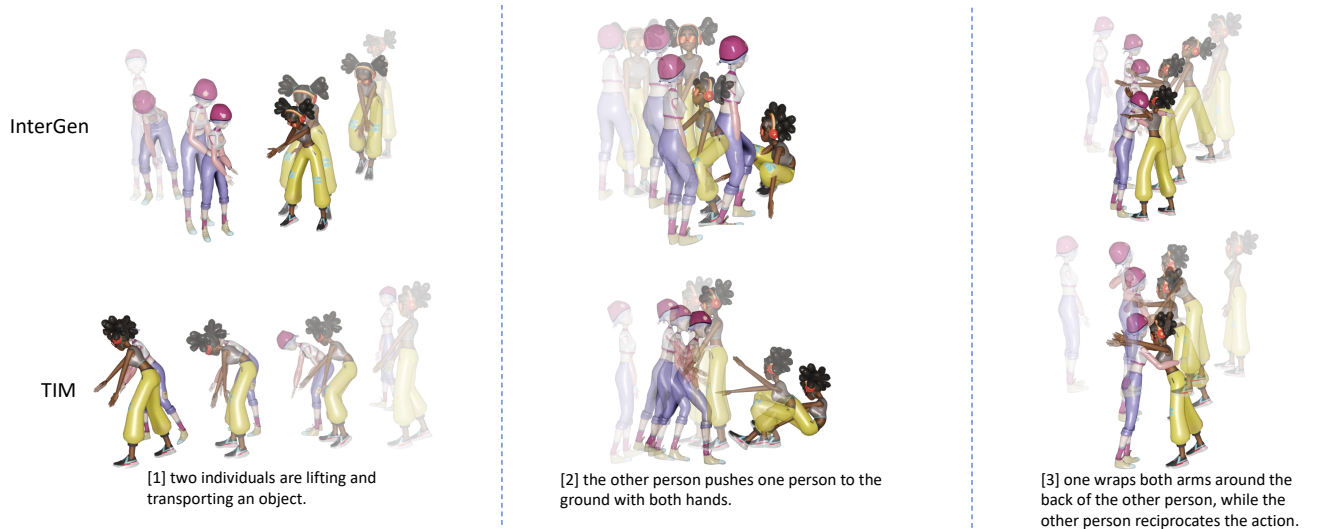


Figure 5: Qualitative comparison with InterGen on human-human motion generation. Darker color indicates later frames.

is set to 1000, and we employ the DDIM (Song, Meng, and Ermon 2020) sampling strategy with 50 timesteps and $\eta = 0$. The cosine noise level schedule (Nichol and Dhariwal 2021) and classifier-free guidance (Ho and Salimans 2022) are adopted, with 10% of random CLIP embeddings set to zero during training and a guidance coefficient of 3.5 during sampling. All the models are trained using the AdamW (Loshchilov and Hutter 2017) optimizer with betas of (0.9, 0.999), a weight decay of 2×10^{-5} , a maximum learning rate of 10^{-4} , and a cosine learning rate schedule with 10 linear warm-up epochs. To balance the contributions of different loss terms, we set $\lambda_{vel} = 30$, $\lambda_{foot} = 30$, $\lambda_{BL} = 10$, $\lambda_{DM} = 3$, $\lambda_{RO} = 0.01$ and $\lambda_{reg} = 1$ in all experiments, as same as InterGen (Liang et al. 2024). We train our diffusion denoisers with a batch size of 256 for 1500 epochs on 8 Nvidia L40S GPUs.

Comparisons with State-of-the-arts

We evaluate our method with state-of-the-art approaches on InterHuman (Liang et al. 2024).

Quantitative Comparisons. Following established practices (Liang et al. 2024), each experiment is conducted 20 times, and the reported metric values represent the mean with a 95% statistical confidence interval. The results on InterHuman are shown in Tab. 7. In comparison to state-of-the-art (SOTA) approaches, our method consistently performs best regarding FID, R-Precision, and MM Dist. For example, our TIM outperforms the previous best motion generation model, InterGen, by 26% in terms of FID, and achieves up to a 35% improvement in R Precision.

Qualitative Comparisons. In Fig. 6, we provide a qualitative comparison between the InterGen and our TIM. It can be seen that motions generated by TIM are more consistent with the description. More visual results are shown in the **supplementary materials**.

Ablation Study and Analysis

In this section, we conduct comprehensive ablation studies to investigate the effectiveness of the key components in TIM, thereby providing a deeper insight into our approach. All experiments are performed on the InterHuman dataset.

Main Ablations. To understand the contribution of each component to the final performance, we incrementally add the proposed modules based on the baseline InterGen (Liang et al. 2024) and present the results in Tab. 2. Initially, we replace self-attention and cross-attention in the transformer with Causal Interactive Injection (CII), which effectively improves both R-Precision and FID while reducing the number of parameters. Next, we apply Role-Evolving Mixing (REM) and yield gains in both R-Precision and FID. It is worth noting that to keep the input feature dimension of RWKV constant, we reduce the dimension of the motion embedding to half of the original, thus also effectively reducing the number of parameters. Finally, when all three methods are applied together, the R-Precision achieves 0.501 and FID achieves 4.702.

CII	REM	LPA	R Precision Top 1↑	FID ↓	Params (M)
			0.371 \pm .010	5.918 \pm .079	182
✓			0.478 \pm .005	5.410 \pm .069	144
✓	✓		0.494 \pm .006	5.019 \pm .077	115
✓	✓	✓	0.501\pm.005	4.702\pm.069	127

Table 2: **Ablation studies on the effectiveness of each component in TIM.** “CII” denotes Causal Interactive Injection, “REM” denotes Role-Evolving Mixing, and “LPA” denotes Localized Pattern Amplification.

Causal Interactive Injection and Role-Evolving Scanning. We ablate the structure of RWKV, Causal Interactive Injection (CII) and Role-Evolving Mixing (REM). The results are shown in Tab. 3. First, to compare the ability of RWKV and the transformer for motion feature extraction, we retained the intrinsic structure of InterGen and only replaced the self-attention from the transformer to RWKV. This resulted in R-Precision and FID of 0.465 and 5.943, respectively. The results show some gain in R-Precision but a decline in FID performance, suggesting that replacing self-attention directly with RWKV is sub-optimal. In contrast, we use CII and REM to change the original motion modeling, and then utilize RWKV’s ability to process motion sequences, which achieve optimal performance. Additionally, we demonstrate the generalizability (0.492 R-Precision and 5.638 FID) of CII and REM by applying CII and REM to the Transformer structure instead of RWKV.

Structure	CII & REM	Cross Attention	R Precision Top 1↑	FID ↓
RWKV	✗	✓	0.465 \pm .005	5.943 \pm .079
Transformer	✓	✗	0.492 \pm .005	5.638 \pm .084
RWKV	✓	✗	0.501\pm.005	4.702\pm.069

Table 3: **Ablation studies on Causal Interactive Injection and Role-Evolving Mixing.** “CII” denotes Causal Interactive Injection and “REM” denotes Role-Evolving Mixing.

Design of Localized Pattern Amplification. In this section, we conduct ablations on the design of Localized Pattern

Amplification (LPA), and the results are shown in Tab. 4. First, we explore the effect of different normalizations on model performance. Using batch normalization (BN) and layer normalization (LN) does not bring gains for text-to-motion tasks. In contrast, AdaLN, which integrates text information into the extraction process of the local motion pattern, proves to be the optimal normalization method. Additionally, we examine how the kernel size of the convolutional layers impacts the model’s performance.

Kernel Size	Norm	R Precision Top 1↑	FID ↓
k=3,1	BN	0.494 \pm .005	5.443 \pm .093
k=3,1	LN	0.488 \pm .005	5.339 \pm .080
k=3,1	AdaLN	0.501\pm.005	4.702\pm.069
k=3,3	AdaLN	0.484 \pm .005	7.120 \pm .090
k=5,1	AdaLN	0.497 \pm .005	5.102 \pm .064

Table 4: **Ablation studies on Localized Pattern Amplification.** “BN” denotes batch normalization, “LN” denotes layer normalization and “AdaLN” denotes adaptive layer normalization. “k=3,1” means that the first kernel size of the convolution is 3 and the second kernel size is 1.

Computational Complexity and Editability.

Computational Complexity. In Tab. 5, we compare our approach with the SOTA method InterGen in terms of computational complexity. TIM requires fewer parameters and FLOPs than InterGen but outperforms it by 1.216 on the comprehensive metric FID. Notably, using only two blocks, TIM has achieved state-of-the-art results with only 32% of InterGen’s trainable parameters and less than 28G FLOPs.

Methods	number blocks	R Precision Top 1↑	FID ↓	Params (M)	Flops (G)
InterGen	8	0.371 \pm .010	5.918 \pm .079	182	80.5
TIM	5	0.501\pm.005	4.702\pm.069	<u>127</u>	<u>58.0</u>
TIM	2	<u>0.494\pm.007</u>	<u>5.424\pm.070</u>	59	27.9

Table 5: Comparison of computational complexity.

Editability. Tab. 6 illustrates that TIM surpasses InterGen in the task of motion in-betweening editing. We perform experiments on the test set of InterHuman and evaluate by generating 80% of the sequences based on the first and last 10% of the sequences. More visual and quantitative results are provided in the **supplementary materials**.

Methods	R Precision Top 1↑	FID ↓	MM Dist↓	Diversity→
InterGen	0.461 \pm .006	4.700 \pm .066	3.780 \pm .001	7.682 \pm .029
TIM	0.516\pm.006	3.590\pm.049	3.760\pm.001	7.795\pm.031

Table 6: Evaluation of motion in-betweening editing task.

Methods	R Precision \uparrow			FID \downarrow	MM Dist \downarrow	Diversity \rightarrow	MModality \uparrow
	Top 1	Top 2	Top 3				
Real	0.441 \pm .005	0.631 \pm .004	0.738 \pm .005	0.001 \pm .0002	3.563 \pm .013	9.000 \pm .083	-
T2M (Guo et al. 2022)	0.325 \pm .004	0.487 \pm .005	0.593 \pm .005	3.342 \pm .0572	4.506 \pm .020	8.535 \pm .055	0.982 \pm .054
InterGen (Liang et al. 2024)	0.400 \pm .006	0.585 \pm .006	0.695 \pm .006	0.475 \pm .0305	3.800 \pm .020	9.095 \pm .055	2.657 \pm .090
TIM(ours)	0.411 \pm .005	0.597 \pm .006	0.707 \pm .004	0.261 \pm .0140	3.737 \pm .015	9.112 \pm .079	2.475 \pm .075

Table 7: **Quantitative evaluation on the InterX (Xu et al. 2024) test set.** We run all the evaluations 20 times. \pm indicates a 95% confidence interval. **Bold** indicates the best result, while underscore refers to the second best.

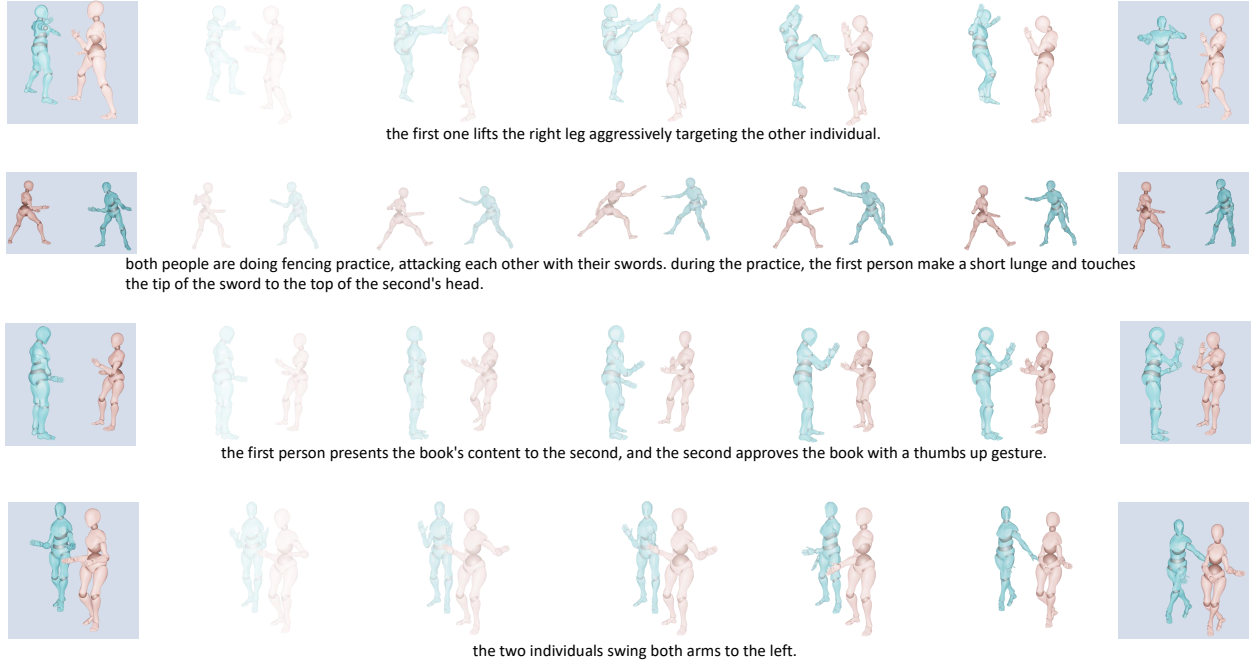


Figure 6: Qualitative results on the motion in-betweening task. The first and last frames are fixed. Darker colors indicate later frames.

Conclusion

In this paper, we introduced TIM (Temporal and Interactive Modeling), a novel and efficient approach for human-human motion generation that leverages RWKV. Our method addresses the limitations of existing transformer-based models by incorporating Causal Interactive Injection to utilize the temporal properties of motion sequences effectively. Additionally, we proposed Role-Evolving Mixing to adapt to the dynamic roles throughout interactions and designed Localized Pattern Amplification to capture short-term motion patterns for generating smoother and more rational motion. Extensive experiments on the InterHuman dataset demonstrate that TIM significantly outperforms existing methods, achieving state-of-the-art results.

Appendix

Experiments on InterX

To demonstrate the generalizability of our approach TIM, we perform corresponding experiments on another large-scale human-human motion generation dataset, InterX (Xu et al. 2024). We maintain the same experimental setup as

described in the paper. Due to the update of InterX, we only report the results of its open-source T2M (Guo et al. 2022). Additionally, we request the reproduction code of the SOTA method InterGen (Liang et al. 2024) from the authors of InterX, and then report the corresponding results.

Following established practices (Liang et al. 2024), each experiment is conducted 20 times, and the reported metric values represent the mean with a 95% statistical confidence interval. The results on InterX are shown in Tab. 7. In comparison to state-of-the-art (SOTA) approaches, our method consistently performs best regarding FID, R-Precision, Diversity, and MM Dist. For example, our TIM outperforms the previous best motion generation model, InterGen, by 45% in terms of FID with fewer parameters.

More Qualitative Results

Human-Human motion generation. We provide the demo in our project.

Motion Editing. Qualitative results on the motion in-betweening task are shown in Fig. 6. Our method achieves smooth and natural transitions between the conditioned and

generated motions while complying with the text.

References

- Ao, T.; Gao, Q.; Lou, Y.; Chen, B.; and Liu, L. 2022. Rhythmic gesticulator: Rhythm-aware co-speech gesture synthesis with hierarchical neural embeddings. *ACM Transactions on Graphics (TOG)*, 41(6): 1–19.
- Bethke, E. 2003. *Game development and production*. Wordware Publishing, Inc.
- Cai, Z.; Jiang, J.; Qing, Z.; Guo, X.; Zhang, M.; Lin, Z.; Mei, H.; Wei, C.; Wang, R.; Yin, W.; et al. 2024. Digital life project: Autonomous 3d characters with social intelligence. In *Proceedings of the IEEE/CVF Conference on Computer Vision and Pattern Recognition*, 582–592.
- Chen, X.; Jiang, B.; Liu, W.; Huang, Z.; Fu, B.; Chen, T.; and Yu, G. 2023. Executing your commands via motion diffusion in latent space. In *Proceedings of the IEEE/CVF Conference on Computer Vision and Pattern Recognition*, 18000–18010.
- Dhariwal, P.; and Nichol, A. 2021. Diffusion models beat gans on image synthesis. *Advances in neural information processing systems*, 34: 8780–8794.
- Duan, Y.; Wang, W.; Chen, Z.; Zhu, X.; Lu, L.; Lu, T.; Qiao, Y.; Li, H.; Dai, J.; and Wang, W. 2024. Vision-rwkv: Efficient and scalable visual perception with rwkv-like architectures. *arXiv preprint arXiv:2403.02308*.
- Fei, Z.; Fan, M.; Yu, C.; Li, D.; and Huang, J. 2024. Diffusion-rwkv: Scaling rwkv-like architectures for diffusion models. *arXiv preprint arXiv:2404.04478*.
- Gong, K.; Lian, D.; Chang, H.; Guo, C.; Jiang, Z.; Zuo, X.; Mi, M. B.; and Wang, X. 2023. Tm2d: Bimodality driven 3d dance generation via music-text integration. In *Proceedings of the IEEE/CVF International Conference on Computer Vision*, 9942–9952.
- Gu, A.; and Dao, T. 2023. Mamba: Linear-time sequence modeling with selective state spaces. *arXiv preprint arXiv:2312.00752*.
- Gu, T.; Yang, K.; An, X.; Feng, Z.; Liu, D.; Cai, W.; and Deng, J. 2024. RWKV-CLIP: A Robust Vision-Language Representation Learner. *arXiv preprint arXiv:2406.06973*.
- Guo, C.; Mu, Y.; Javed, M. G.; Wang, S.; and Cheng, L. 2024. Momask: Generative masked modeling of 3d human motions. In *Proceedings of the IEEE/CVF Conference on Computer Vision and Pattern Recognition*, 1900–1910.
- Guo, C.; Zou, S.; Zuo, X.; Wang, S.; Ji, W.; Li, X.; and Cheng, L. 2022. Generating diverse and natural 3d human motions from text. In *Proceedings of the IEEE/CVF Conference on Computer Vision and Pattern Recognition*, 5152–5161.
- Guo, C.; Zuo, X.; Wang, S.; Zou, S.; Sun, Q.; Deng, A.; Gong, M.; and Cheng, L. 2020. Action2motion: Conditioned generation of 3d human motions. In *Proceedings of the 28th ACM International Conference on Multimedia*, 2021–2029.
- Habibie, I.; Elgharib, M.; Sarkar, K.; Abdullah, A.; Nyatsanga, S.; Neff, M.; and Theobalt, C. 2022. A motion matching-based framework for controllable gesture synthesis from speech. In *ACM SIGGRAPH 2022 conference proceedings*, 1–9.
- He, Q.; Zhang, J.; Peng, J.; He, H.; Wang, Y.; and Wang, C. 2024. PointRWKV: Efficient RWKV-Like Model for Hierarchical Point Cloud Learning. *arXiv preprint arXiv:2405.15214*.
- Ho, J.; Jain, A.; and Abbeel, P. 2020. Denoising diffusion probabilistic models. *Advances in neural information processing systems*, 33: 6840–6851.
- Ho, J.; and Salimans, T. 2022. Classifier-free diffusion guidance. *arXiv preprint arXiv:2207.12598*.
- Hochreiter, S.; and Schmidhuber, J. 1997. Long short-term memory. *Neural computation*, 9(8): 1735–1780.
- Liang, H.; Zhang, W.; Li, W.; Yu, J.; and Xu, L. 2024. Inter-gen: Diffusion-based multi-human motion generation under complex interactions. *International Journal of Computer Vision*, 1–21.
- Loshchilov, I.; and Hutter, F. 2017. Decoupled weight decay regularization. *arXiv preprint arXiv:1711.05101*.
- Magnenat-Thalmann, N.; Thalmann, D.; Magnenat-Thalmann, N.; and Thalmann, D. 1985. *Computer animation*. Springer.
- Nichol, A. Q.; and Dhariwal, P. 2021. Improved denoising diffusion probabilistic models. In *International conference on machine learning*, 8162–8171. PMLR.
- Parent, R. 2012. *Computer animation: algorithms and techniques*. Newnes.
- Peng, B.; Alcaide, E.; Anthony, Q.; Albalak, A.; Arcadinho, S.; Biderman, S.; Cao, H.; Cheng, X.; Chung, M.; Grella, M.; et al. 2023. Rwkv: Reinventing rnns for the transformer era. *arXiv preprint arXiv:2305.13048*.
- Petrovich, M.; Black, M. J.; and Varol, G. 2021. Action-conditioned 3d human motion synthesis with transformer vae. In *Proceedings of the IEEE/CVF International Conference on Computer Vision*, 10985–10995.
- Petrovich, M.; Black, M. J.; and Varol, G. 2022. TEMOS: Generating diverse human motions from textual descriptions. In *European Conference on Computer Vision*, 480–497. Springer.
- Pinyoanuntapong, E.; Wang, P.; Lee, M.; and Chen, C. 2024. Mmm: Generative masked motion model. In *Proceedings of the IEEE/CVF Conference on Computer Vision and Pattern Recognition*, 1546–1555.
- Radford, A.; Kim, J. W.; Hallacy, C.; Ramesh, A.; Goh, G.; Agarwal, S.; Sastry, G.; Askell, A.; Mishkin, P.; Clark, J.; et al. 2021. Learning transferable visual models from natural language supervision. In *International conference on machine learning*, 8748–8763. PMLR.
- Saridis, G. 1983. Intelligent robotic control. *IEEE Transactions on Automatic Control*, 28(5): 547–557.
- Shafir, Y.; Tevet, G.; Kapon, R.; and Bermano, A. H. 2023. Human motion diffusion as a generative prior. *arXiv preprint arXiv:2303.01418*.
- Song, J.; Meng, C.; and Ermon, S. 2020. Denoising diffusion implicit models. *arXiv preprint arXiv:2010.02502*.

- Tanaka, M.; and Fujiwara, K. 2023. Role-aware interaction generation from textual description. In *Proceedings of the IEEE/CVF international conference on computer vision*, 15999–16009.
- Tevet, G.; Gordon, B.; Hertz, A.; Bermano, A. H.; and Cohen-Or, D. 2022a. Motionclip: Exposing human motion generation to clip space. In *European Conference on Computer Vision*, 358–374. Springer.
- Tevet, G.; Raab, S.; Gordon, B.; Shafir, Y.; Cohen-Or, D.; and Bermano, A. 2022b. Human motion diffusion model. *arXiv preprint arXiv:2209.14916*.
- Urbain, J. 2010. Introduction to game development. *Cell*, 414: 745–5102.
- Van Den Oord, A.; Vinyals, O.; et al. 2017. Neural discrete representation learning. *Advances in neural information processing systems*, 30.
- Vaswani, A. 2017. Attention is all you need. *arXiv preprint arXiv:1706.03762*.
- Wang, S.; Zhao, X.; Xu, H.-M.; Chen, Z.; Yu, D.; Chang, J.; Yang, Z.; and Zhao, F. 2023a. Towards domain generalization for multi-view 3d object detection in bird-eye-view. In *Proceedings of the IEEE/CVF Conference on Computer Vision and Pattern Recognition*, 13333–13342.
- Wang, Z.; Wang, J.; Lin, D.; and Dai, B. 2023b. Intercontrol: Generate human motion interactions by controlling every joint. *arXiv preprint arXiv:2311.15864*.
- Xu, L.; Lv, X.; Yan, Y.; Jin, X.; Wu, S.; Xu, C.; Liu, Y.; Zhou, Y.; Rao, F.; Sheng, X.; et al. 2024. Inter-x: Towards versatile human-human interaction analysis. In *Proceedings of the IEEE/CVF Conference on Computer Vision and Pattern Recognition*, 22260–22271.
- Yang, Z.; Zhang, H.; Zhao, D.; Wei, B.; and Xu, Y. 2024. Restore-RWKV: Efficient and Effective Medical Image Restoration with RWKV. *arXiv preprint arXiv:2407.11087*.
- Yuan, H.; Li, X.; Qi, L.; Zhang, T.; Yang, M.-H.; Yan, S.; and Loy, C. C. 2024. Mamba or RWKV: Exploring High-Quality and High-Efficiency Segment Anything Model. *arXiv preprint arXiv:2406.19369*.
- Zhang, J.; Zhang, Y.; Cun, X.; Zhang, Y.; Zhao, H.; Lu, H.; Shen, X.; and Shan, Y. 2023a. Generating human motion from textual descriptions with discrete representations. In *Proceedings of the IEEE/CVF conference on computer vision and pattern recognition*, 14730–14740.
- Zhang, M.; Cai, Z.; Pan, L.; Hong, F.; Guo, X.; Yang, L.; and Liu, Z. 2024a. Motiondiffuse: Text-driven human motion generation with diffusion model. *IEEE Transactions on Pattern Analysis and Machine Intelligence*.
- Zhang, M.; Guo, X.; Pan, L.; Cai, Z.; Hong, F.; Li, H.; Yang, L.; and Liu, Z. 2023b. Remodiffuse: Retrieval-augmented motion diffusion model. In *Proceedings of the IEEE/CVF International Conference on Computer Vision*, 364–373.
- Zhang, M.; Li, H.; Cai, Z.; Ren, J.; Yang, L.; and Liu, Z. 2024b. Finemogen: Fine-grained spatio-temporal motion generation and editing. *Advances in Neural Information Processing Systems*, 36.
- Zhong, C.; Hu, L.; Zhang, Z.; and Xia, S. 2023. Att2m: Text-driven human motion generation with multi-perspective attention mechanism. In *Proceedings of the IEEE/CVF International Conference on Computer Vision*, 509–519.